Journal of Computational Physics 374 (2018) 1261–1266

Contents lists available at ScienceDirect

Journal of Computational Physics

www.elsevier.com/locate/jcp

Short note

Boundary optimized diagonal-norm SBP operators

Ken Mattsson [a,*], Martin Almquist [b,a], Edwin van der Weide [c]

[a] Uppsala University, Department of Information Technology, PO Box 337, S-751 05 Uppsala, Sweden
[b] Department of Geophysics, Stanford University, Stanford, CA 94305, United States
[c] Department of Mechanical Engineering, University of Twente, the Netherlands

ARTICLE INFO

Article history:
Received 10 April 2018
Received in revised form 14 May 2018
Accepted 2 June 2018
Available online 5 June 2018

Keywords:
Finite difference methods
Boundary treatment
High order accuracy
Stability
Euler equations

ABSTRACT

By using non-equispaced grid points near boundaries, we derive boundary optimized first derivative finite difference operators, of orders up to twelve. The boundary closures are based on a diagonal-norm summation-by-parts (SBP) framework, thereby guaranteeing linear stability on piecewise curvilinear multi-block grids. The new operators lead to significantly more efficient numerical approximations, compared with traditional SBP operators on equidistant grids. We also show that the non-uniform grids make it possible to derive operators with fewer one-sided boundary stencils than their traditional counterparts. Numerical experiments with the 2D compressible Euler equations on a curvilinear multi-block grid demonstrate the accuracy and stability properties of the new operators.

1. Introduction

Energy-stable numerical methods for partial differential equations (PDEs) often rely on a summation-by-parts (SBP) property. The SBP property ensures that the discrete differential operators mimic the integration-by-parts formula for their continuous counterparts. Examples of discrete operators with the SBP property include some finite difference (FD), spectral collocation [1,2], and finite volume methods [3]. In this article, we focus exclusively on finite difference operators. SBP FD operators [4–6] are routinely combined with the simultaneous approximation term (SAT) method to impose boundary conditions.

Traditional SBP FD operators found in the literature are essentially central finite difference stencils, defined on regular grids, closed at the boundaries with one-sided difference stencils (independent of the grid-size) that preserve the SBP-property. Every SBP FD operator is associated with a quadrature rule that defines an inner product—and hence a norm—on the space of discrete solution vectors. The structure of the norm matrix is important; for problems with curvilinear grids, only diagonal norm matrices facilitate provably stable schemes. Hence, diagonal-norm SBP operators are the obvious choice in many applications. Unfortunately, however, traditional diagonal-norm SBP operators suffer from reduced order of accuracy near boundaries. It has been shown that diagonal-norm SBP operators where all FD stencils have accuracy at least p are associated with a quadrature rule of degree at least $2p-1$ [7]. Moreover, if the repeating interior stencil is of order $2p$, the order of the boundary closure may not exceed p [4], assuming uniform grids. In a recent study [8] this fact has been proven to hold also for grids with arbitrary point distributions near domain boundaries. For first order hyperbolic equations, this limits the global convergence rate to $(p+1)$th order [9].

* Corresponding author.
E-mail addresses: ken.mattsson@it.uu.se (K. Mattsson), malmquist@stanford.edu (M. Almquist), e.t.a.vanderweide@utwente.nl (E. van der Weide).

https://doi.org/10.1016/j.jcp.2018.06.010
0021-9991/

In an effort to improve the accuracy of first-derivative diagonal-norm SBP operators, [10] introduced a type of boundary optimized operators, of orders up to eight. In the construction of the operators, the authors allowed for a few non-equispaced grid points near the boundaries. This approach introduces more free parameters that can be tuned for accuracy. The grid point locations, as well as the coefficients of the operator, are obtained by solving a non-linear constrained optimization problem where the leading order truncation error coefficients are used as objective function. Although the optimized $2p$th-order operators were closed with pth-order accurate boundary stencils just like their traditional counterparts, the leading order error constants were reduced by several orders of magnitude. Numerical experiments indicate that this can lead to large gains in the pre-asymptotic convergence regime.

In a recent paper [11] the existence of traditional diagonal-norm SBP operators up to order $2p = 30$ is proven. It turns out that the minimum number of boundary stencils grows quickly with the order of accuracy; operators of orders $2p = 10, 12, 30$, require 11, 14, 71 boundary stencils, respectively. Wide boundary stencils impact the usefulness of the operators in multi-block configurations where some blocks may be small and the operators will not fit unless an excessively fine grid is introduced. Further, the number of free parameters that remain after imposing the SBP property and pth order boundary accuracy tends to increase rapidly with p. It is important to choose the free parameters well, since they affect the leading-order error constants of the boundary stencils and the spectral radius of the operator. Naturally, this optimization problem becomes more cumbersome as the number of free parameters increases. For $2p \geq 8$ there is the additional difficulty that some of the parameters reside in the norm matrix so that the condition of positive definiteness constrains the optimization problem.

In [10] the mathematical software *Maple* was utilized to solve the non-linear constrained optimization problem. Due to a limitation in Maple, the optimization problem could however only be solved with at most 3 non-equidistant grid-points and at most 8 boundary points. The present study revisits the optimization problem. By using the numerical optimization software *SNOPT 7.2* [12] developed at Stanford University, we are able to improve the previous work. The main results are twofold: First, we derive up to 12th order boundary optimized operators. Second, we derive $2p$th order diagonal-norm SBP operators with less than $2p$ boundary points, which for $p > 1$ is impossible for traditional operators on equidistant grids. For example: a 12th order optimized operator with only 10 boundary points is derived. Remarkably, the boundary-optimized operators do not introduce stiffness; the spectral radii are almost identical to those of the corresponding traditional operators.

In Section 2 the SBP definitions are introduced. In Section 3, the newly derived SBP operators are applied to the 2D Euler equations on a curvilinear multi-block domain. Section 4 summarizes the work. The coefficients of the optimized operators are included online as supplementary data for this paper, as described in Appendix A.

2. Definitions

The domain $(0 \leq x \leq L)$ is discretized using m grid points:

$$\mathbf{x} = [x_1, x_2, \ldots, x_{m-1}, x_m]^T ,$$

i.e., $\mathbf{x}$ denotes a vector holding the grid-points. For an equidistant grid we have

$$x_i = (i-1)\,h, \quad i = 1, 2, \ldots, m, \quad h = \tfrac{L}{m-1} .$$

In the present study we will allow up to 6 grid-points (depending on the order of accuracy) near the boundary to be non-equispaced, to improve accuracy. We will use the standard l^2 inner product for vectors $\mathbf{u}, \mathbf{v} \in \mathbf{R}^m$, i.e. $(\mathbf{u}, \mathbf{v})_h = h\mathbf{u}^T\mathbf{v}$. The following definition (first stated in [13]) is relevant to the present study:

Definition 2.1. An explicit $2pth$-order accurate finite difference scheme with minimal stencil width for the Cauchy problem is denoted a $2pth$-order accurate narrow-stencil.

2.1. SBP operators

The SBP definitions can be found in earlier papers (see for example [4]). For completeness we restate them below for the first derivative:

Definition 2.2. A difference operator $D_1 = H^{-1}Q$, approximating $\partial/\partial x$ using a repeated narrow-stencil in the interior, is said to be a diagonal-norm first-derivative SBP operator if H is diagonal and positive definite, and $Q + Q^T = diag(-1, 0, \ldots, 0, 1)$.

Let $\mathbf{x}^k$ denote the projection of the polynomial $\frac{x^k}{k!}$ onto the grid. We will use the convention that $\mathbf{x}^0 = [1, 1, \ldots, 1]^T$ and $\mathbf{x}^{-1} = [0, 0, \ldots, 0]^T$. The following definition (first stated in [10]) is central to the present study.

Definition 2.3. We say that the diagonal-norm first-derivative SBP operator D_1 is $2pth$-order if the error vector $\mathbf{err}_k = H\mathbf{x}^{k-1} - Q\,\mathbf{x}^k$ vanishes for $k = 0, \ldots, 2\,p$ in the interior and for $k = 0, \ldots, p$ near the boundaries.

Table 1
The number of boundary stencils, comparing the Traditional and optimized SBP operators (both Accurate and Minimal) for $2p = 4, 6, 8, 10, 12$. We list the number of boundary points and the number of non-uniform grid spacings in parenthesis for the optimal SBP operators.

	Traditional	Minimal	Accurate
4th order	4	3 (1)	4 (2)
6th order	6	5 (2)	7 (4)
8th order	8	6 (2)	8 (4)
10th order	11	8 (3)	10 (5)
12th order	15	10 (4)	12 (6)

Remark. A $2pth$-order diagonal-norm first-derivative SBP operator is restricted to pth-order accuracy (see [4]) at the boundaries, i.e., $\mathbf{err}_{p+1}$ is the leading order error. This implies [9,14] that the convergence rate drops to $(p+1)th$ order for first order hyperbolic problems, and $(p+2)th$ order for parabolic and second order hyperbolic problems, assuming null-space consistency.

In the traditional first-derivative SBP operators used in the present study, the free parameters have been carefully chosen to minimize the discrete l^2-norm of the leading order boundary error, $\|\mathbf{err}_{p+1}\|_h^2$ for the $2pth$ order case. The spectral radii of the operators are also small. In fact, [13] found a strong correlation between small leading order truncation error and small spectral radius. Hence, by minimizing the norm of the leading order truncation error one can expect to also minimize the spectral radius of the operator.

2.2. Optimized diagonal-norm SBP operators

To improve the accuracy of traditional diagonal-norm operators we allow for non-uniform grid point distributions near boundaries. Let the domain be the interval $[0, L]$ and consider the case with n non-uniform grid spacings. We introduce d_i, $i = 1, \ldots, n$, such that $h\,d_i$ is the distance between the ith and $(i+1)$th grid point. We also introduce the notation $\xi_j = \sum_{i=1}^{j} d_i$, $j = 1, \ldots, n$. The grid-spacing in the interior is given by $h = L/(2\,\xi_n + (m - 2n - 1))$, where m is the number of grid points. The grid points are thus

$$\mathbf{x} = [0,\ \xi_1 h,\ \xi_2 h,\ \ldots,\ \xi_n h,\ (\xi_n + 1)h,\ \ldots,\ (\xi_n + m - 2n - 2)h,\ L - \xi_n h,\ L - \xi_{n-1} h,\ \ldots,\ L - \xi_1 h,\ L]\,.$$

The unknowns in the optimization are the distances d_i and the coefficients in H and Q. For more details we refer to [10].

In the present study, optimized $4th$, $6th$, $8th$, $10th$ and $12th$ order diagonal-norm SBP operators have been constructed. Because the objective function may contain many local minima, we can not guarantee that the constructed operators correspond to global minima. Furthermore, it is not obvious how to choose the objective function. We have observed that it is often beneficial to include a linear combination of the two leading order errors, i.e. to minimize $\|\mathbf{err}_{p+1}\|_h^2 + \|\mathbf{err}_{p+2}\|_h^2$ rather than $\|\mathbf{err}_{p+1}\|_h^2$.

We have constructed two kinds of optimized operators. The first kind has the minimum number of boundary points that is required to achieve pth order accuracy at the boundary. This kind will be referred to as *Minimal*. The second kind of operators have been constructed to have the best possible accuracy properties and will be referred to as *Accurate*. The Accurate operators typically have a few more boundary points than the corresponding Minimal operators. Table 1 compares the number of boundary points for Traditional, Minimal, and Accurate operators of orders four to twelve. We also list the number of non-uniform grid spacings n for the optimized operators. In general, for interior order $2p$ and r boundary stencils, $n = r - p$, as the grid points that are touched by the interior stencil must remain equispaced.

3. The Euler vortex problem

To test the accuracy properties of the optimized operators we consider the nonlinear Euler equations in curvilinear coordinates formulated in conservative form,

$$J\mathbf{u}_t + \tilde{\mathbf{F}}_\xi + \tilde{\mathbf{G}}_\eta = 0\,, \tag{1}$$

where ξ and η are the spatial coordinates in the reference domain and

$$\mathbf{u} = \begin{bmatrix} \rho \\ \rho u \\ \rho v \\ e \end{bmatrix}, \quad \tilde{\mathbf{F}} = \begin{bmatrix} \rho U \\ \rho u U + y_\eta p \\ \rho v U - x_\eta p \\ (e+p)U \end{bmatrix}, \quad \tilde{\mathbf{G}} = \begin{bmatrix} \rho V \\ \rho u V - y_\xi p \\ \rho v V + x_\xi p \\ (e+p)V \end{bmatrix}.$$

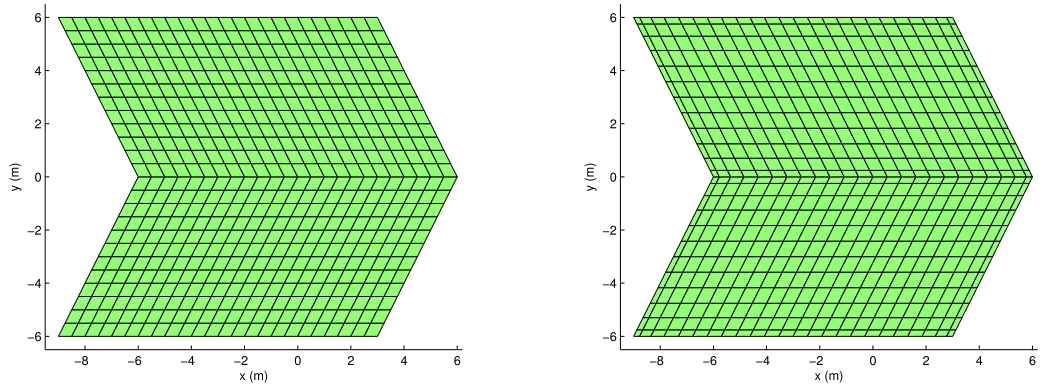

(a) Grid for Traditional operators (b) Grid for the Accurate 8th order operator

Fig. 1. The computational domain, consisting of 2 curvilinear grids, with discontinuous metrics along the interface. Here with 21×11 grid-points in each domain.

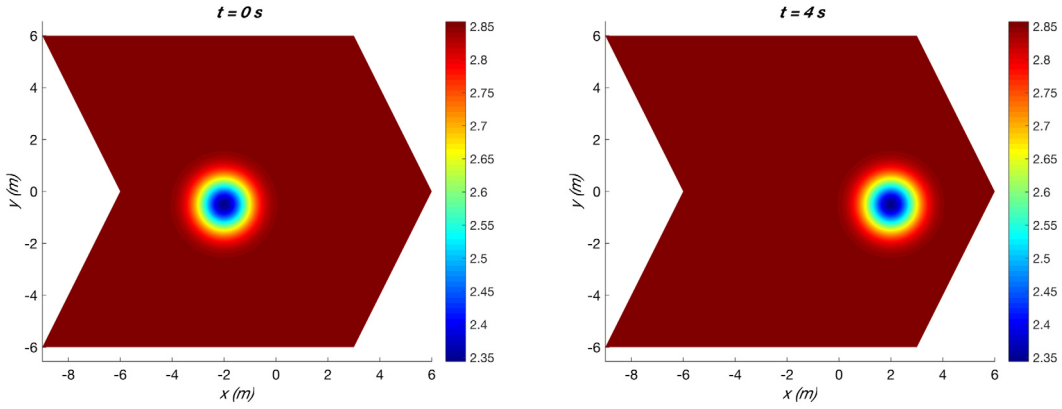

(a) Initial data (b) Exact solution at $t = 4$ s

Fig. 2. The pressure component of the exact solution at times $t = 0$ s and $t = 4$ s. $M = 0.5$ and $\epsilon = 4$.

Here x and y are the coordinates in the physical domain and

$$J = x_\xi y_\eta - x_\eta y_\xi \ , \ U = y_\eta u - x_\eta v \ , \ V = -y_\xi u + x_\xi v \ .$$

Further, ρ is the density (scaled to free stream density ρ_∞); u, v are the velocity components in the x, y directions respectively (scaled to free stream speed of sound c_∞); $e = e_i + \frac{\rho}{2}(u^2 + v^2)$ is the total energy (nondimensionalized with respect to $\rho_\infty c_\infty^2$) and e_i is the internal energy. Pressure is obtained from the equation of state for an ideal gas: $p = (\gamma - 1)e_i$.

In the experiments below we consider the propagation of a vortex that satisfies (1). The analytic vortex solution is steady in the frame of reference moving with the free-stream. (See [10] for the analytic solution in Cartesian coordinates.) The vortex is introduced into the computational domain by using the analytic solution as boundary data and initial data. We consider a domain that requires a two-block discretization (see Fig. 1) and use SATs to couple the two blocks along the interface. Details concerning how to discretize this problem with the SBP-SAT method can be found in [10]. Note that the boundary stencils of the operators are used along the block interface in both blocks, as well as near the domain boundaries. Fig. 1a shows the grid used by the Traditional operators, while Fig. 1b shows the grid used by the Accurate 8th order operator.

3.1. Convergence study

The initial position of the center of the vortex is $(x, y) = (-2, -0.5)$, so that the block interface cuts the vortex (see Fig. 2). The vortex is then propagated to the right along the grid interface a distance of 4 units (corresponding to $t = 4$) where we measure the l^2-error in the pressure component. For the time-integration we use a 6th-order accurate Runge–Kutta method [15] with $\Delta t = 0.001$, to guarantee that temporal errors are small. We set $M = 0.5$ and $\epsilon = 4$. (Here ϵ is a parameter that governs the vortex strength and M is the Mach number, see [10].)

In Tables 2, 3, 4 we present convergence results using Traditional and optimized SBP operators, of orders 4, 6, 8, 10 and 12. Here we include both the Minimal and Accurate operators.

Table 2
$log(l^2 - errors)$, denoted Err, and convergence rates q, for SBP operators of orders 4 and 6. Comparing the Traditional, Minimal, and Accurate operators.

	Traditional 4		Minimal 4		Accurate 4		Traditional 6		Minimal 6		Accurate 6	
N	Err	q	Err	q	Err	q	Err	q	Err	q	Err	q
31	−3.27		−3.77		−4.08		−2.90		−4.34		−4.63	
61	−4.27	3.32	−4.76	3.29	−5.16	3.58	−4.15	4.13	−5.71	4.55	−6.23	5.29
91	−4.83	3.16	−5.32	3.19	−5.79	3.58	−5.01	4.91	−6.46	4.30	−7.04	4.60
121	−5.22	3.10	−5.72	3.13	−6.24	3.60	−5.65	5.08	−6.99	4.22	−7.57	4.29
161	−5.60	3.07	−6.10	3.09	−6.68	3.59	−6.29	5.13	−7.51	4.17	−8.09	4.18

Table 3
$log(l^2 - errors)$, denoted Err, and convergence rates q, for SBP operators of orders 8 and 10. Comparing the Traditional, Minimal, and Accurate operators.

	Traditional 8		Minimal 8		Accurate 8		Traditional 10		Minimal 10		Accurate 10	
N	Err	q	Err	q	Err	q	Err	q	Err	q	Err	q
31	−2.95		−4.76		−5.30		−2.86		−3.94		−5.45	
61	−4.28	4.42	−6.34	5.26	−7.35	6.82	−4.26	4.66	−5.72	5.90	−7.61	7.16
91	−5.12	4.77	−7.23	5.00	−8.47	6.33	−5.27	5.71	−6.84	6.41	−9.06	8.22
121	−5.71	4.77	−7.85	5.00	−9.22	5.99	−5.98	5.74	−7.68	6.70	−10.07	8.14
161	−6.33	4.93	−8.48	5.00	−9.95	5.84	−6.70	5.75	−8.53	6.82	−11.05	7.81

Table 4
$log(l^2 - errors)$, denoted Err, and convergence rates q, for SBP operators of order 12. Comparing the Traditional, Minimal, and Accurate operators.

	Traditional 12		Minimal 12		Accurate 12	
N	Err	q	Err	q	Err	q
31	−2.32		−4.70		−5.30	
61	−3.52	4.01	−6.73	6.74	−7.65	7.81
91	−5.15	9.22	−8.17	8.19	−9.41	10.03
121	−5.98	6.68	−9.25	8.64	−10.88	11.71
161	−6.82	6.66	−10.16	7.29	−12.28	11.23

3.2. Long-time simulations

To illustrate the importance of improved boundary accuracy for long-time simulations we modify the problem in Section 3.1. Instead of imposing the exact solution as boundary data on all of the outer boundaries, we couple the left and right boundaries using SATs. As the vortex leaves the domain through the right boundary it re-enters on the left. One revolution takes 12 s so that at every integer multiple of 12 s, the exact solution is identical to the initial data. We set $M = 0.5$ and $\epsilon = 2$.

Fig. 3 compares the Traditional and Accurate 12th order operators by presenting the pressure component after one revolution (Traditional) and after four revolutions (Accurate). Both simulations use $m = 51 \times 101$ grid points in each sub-block and the time step $\Delta t = 0.004$. With the Traditional operator, the vortex is visibly distorted (already at $t = 12$), whereas it keeps its shape (even at $t = 48$) when the Accurate operator is used.

Remark. A numerical study, not presented here, comparing the Traditional and the optimized (Minimal and Accurate) operators shows that the optimized and traditional SBP operators have almost identical spectral radii, and hence identical stability restrictions on the time-step.

4. Conclusion

We have utilized non-uniform grid point distributions near boundaries to construct boundary optimized diagonal-norm SBP operators for the first derivative. The first main result is the construction of optimized operators of orders up to twelve. While the order of accuracy near the boundaries is no higher than for traditional diagonal-norm operators, the leading order error constants are much smaller. Numerical experiments with the 2D compressible Euler equations show that the optimized operators can yield several orders of magnitude more accurate results than the traditional versions. While the performance of the optimized operators is somewhat problem-dependent, they frequently exhibit higher convergence rates than the expected $(p+1)$th order down to relative errors of 10^{-10}. In the limit $h \to 0$, however, we expect the convergence rates to approach $(p+1)$th order.

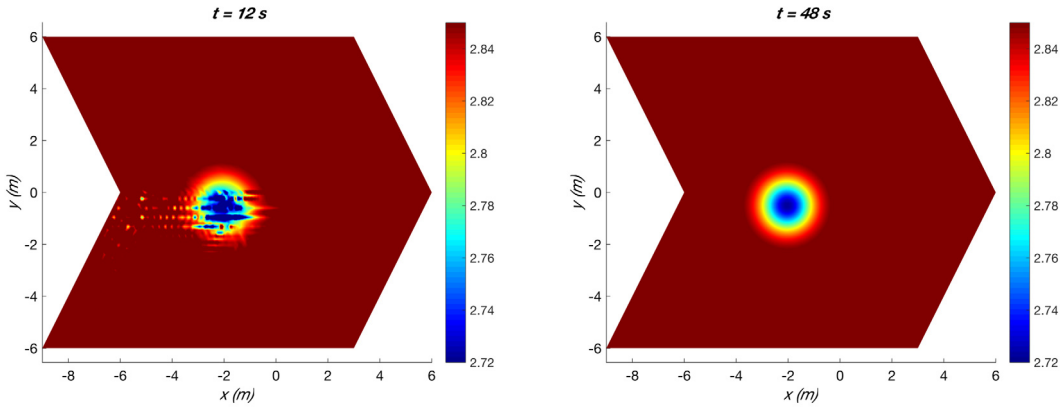

(a) Traditional 12th order (b) Accurate 12th order

Fig. 3. Pressure component of the solution at $t = 12$ s (one revolution) using Traditional and at $t = 48$ s (four revolutions) using Accurate 12th order operators with $m = 51 \times 101$ grid-points in each sub-block.

The second main result is the construction of $2p$th order diagonal-norm SBP operators with less than $2p$ boundary points, which is the lower limit for traditional SBP operators on equidistant grids.

Acknowledgements

M. Almquist gratefully acknowledges support from the Knut and Alice Wallenberg Foundation (Dnr. KAW 2016.0498) during the later stages of this work.

Appendix A. SBP operators

The Accurate, Minimal and Traditional diagonal-norm SBP operators used in Section 3 are available online as MATLAB function files at https://bitbucket.org/martinalmquist/optimized_sbp_operators. The Matlab functions return the differentiation matrix D_1, the norm matrix H, the grid point vector $\mathbf{x}$, and the interior grid spacing h. Input to the functions are the grid size m and the width L of the domain.

References

[1] M.H. Carpenter, D. Gottlieb, Spectral methods on arbitrary grids, J. Comput. Phys. 129 (1996) 74–86.
[2] M.H. Carpenter, T.C. Fisher, E.J. Nielsen, S.H. Frankel, Entropy stable spectral collocation schemes for the Navier–Stokes equations: discontinuous interfaces, SIAM J. Sci. Comput. 36 (2014) B835–B867.
[3] M. Svärd, J. Nordström, Stability of finite volume approximations for the Laplacian operator on quadrilateral and triangular grids, Appl. Numer. Math. 51 (1) (2004) 101–125.
[4] H.-O. Kreiss, G. Scherer, Finite element and finite difference methods for hyperbolic partial differential equations, Mathematical Aspects of Finite Elements in Partial Differential Equations, Academic Press, New York, 1974.
[5] K. Mattsson, J. Nordström, Summation by parts operators for finite difference approximations of second derivatives, J. Comput. Phys. 199 (2) (2004) 503–540.
[6] M. Svärd, J. Nordström, Review of summation-by-parts-operators schemes for initial-boundary-value problems, J. Comput. Phys. 268 (2014) 17–38.
[7] J. Hicken, D. Zingg, Summation-by-parts operators and high-order quadrature, J. Comput. Appl. Math. 237 (2013) 111–125.
[8] V. Linders, T. Lundquist, J. Nordström, On the order of accuracy of finite difference operators on diagonal norm based summation-by-parts form, SIAM J. Numer. Anal. 56 (2) (2018) 1048–1063.
[9] M. Svärd, J. Nordström, On the order of accuracy for difference approximations of initial-boundary value problems, J. Comput. Phys. 218 (2006) 333–352.
[10] K. Mattsson, M. Almquist, M.H. Carpenter, Optimal diagonal-norm SBP operators, J. Comput. Phys. 264 (2014) 91–111.
[11] N. Albin, J. Klarmann, An algorithmic exploration of the existence of high-order summation by parts operators with diagonal norm, J. Sci. Comput. 69 (2016) 633–650.
[12] P.E. Gill, W. Murray, M.A. Saunders, Snopt: an sqp algorithm for large-scale constrained optimization, SIAM Rev. 47 (2005) 99–131.
[13] K. Mattsson, M. Svärd, M. Shoeybi, Stable and accurate schemes for the compressible Navier–Stokes equations, J. Comput. Phys. 227 (4) (2008) 2293–2316.
[14] M. Svärd, J. Nordström, On the Convergence Rates of Energy-Stable Finite-Difference Schemes, Technical Report 2017:14, Linköping University, 2017.
[15] E.A. Alshinaa, E.M. Zaksb, N.N. Kalitkin, Optimal first- to sixth-order accurate Runge–Kutta schemes, Comput. Math. Math. Phys. 48 (2008) 418–429.